**EUROPEAN ORGANIZATION FOR NUCLEAR RESEARCH**

CERN – PS DIVISION

**PS/RF/Note 2000-004**

# IMPEDANCE MEASUREMENT OF THE SPS MKE KICKER BY MEANS OF THE COAXIAL WIRE METHOD

**F. Caspers, C. Gonzalez, M. D'yachkov, E. Shaposhnikova, H. Tsutsui**

**Abstract**

In this paper we present beam coupling impedance measurements obtained by the well known coaxial wire method, for the SPS MKE kicker. This data together with the measured beam spectrum is used to estimate the heat deposition and this is then compared with the directly measured heat deposition in a spare MKE kicker tank placed in the SPS ring. The frequency dependent real and imaginary parts of the distributed impedance are obtained from the measured S-parameters by standard and improved "log-formulae". The calculation of the different beam current spectral components as well as the measured raw and processed data for the MKE kicker impedance are shown.

Geneva, Switzerland

February 9, 2000

# 1 MKE Impedance Measurements

Using the standard single wire measurement technique a number of transmission measurements were carried out on the SPS MKE kicker. For practical reasons we used flat flanges at the MKE kicker beam pipe port (no conical transitions) and the diameter of the thin wire was 0.4 mm. In order to improve the matching of this wire (seen from inside the tank with respect to the 50 $\Omega$ coaxial cable) resistors were installed near either flange of the tank. The ohmic value $R$ of these low inductance carbon resistors is simply determined by the relation: R = $Z_c$ - 50 $\Omega$. The approximate characteristic impedance $Z_c$ of a thin wire in the ferrite loaded structure (Fig. 1) is determined assuming the model of a wire between two parallel conducting plates by using the relation

$$Z_{c1} = 60\ \ln[1.27\,\frac{D}{d}] \tag{1}$$

For the vertical aperture D = 32 mm (horizontal aperture is 140 mm) and the wire diameter d = 0.4 mm the value of characteristic impedance $Z_{c1}$ is about 270 $\Omega$.

The choice of the geometry indicated above is somewhat arbitrary and one may argue that it would be more suitable to refer to the same wire in a beam pipe with a 100 mm diameter. In that case the characteristic impedance $Z_{c2}$ calculated using a classical formula for the coaxial line is

$$Z_{c2} = 60\ \ln[\frac{D}{d}] \tag{2}$$

and we find $Z_{c2}$ = 330 $\Omega$. The difference between the two values is less than $20\%$ and not considered to be significant for the present measurements. A simplified cross-section of this kicker is given in Fig. 1.

The raw data obtained using the HP-8753D network analyzer are shown in Figs. 2-5. In each case a connecting cable calibration (response calibration) has been repeated and each measurement contains 801 points. The geometrical length of the kicker between the coaxial connectors was accurately measured. This length ($l = 2.2253$ m) has been taken into account via the electrical delay correction function in the network analyzer and was subtracted in the phase display.

Correction procedures were subsequently applied on both amplitude and phase data and are shown in Figs. 6-8. For the amplitude (modulus) of $S_{21}$ ($S_{21}$ = $S_{12}$) we had to subtract the losses attributed to the matching resistor, which were simply obtained by taking the attenuation values at the lowest frequency point (around 100 kHz). This correction amounts approximately to 15 dB. It appears as the vertical distance between the dashed an the solid lines shown in the Figs. 6-8.

For the phase plots we had to remove the network analyzer display related phase ambiguities of $360^\circ$, and the procedure is most evident from Fig. 7. Note that all the resonances lead to fast phase variations vs. frequency. These fast variations may coincide and may be mistaken for $360^\circ$ phase jumps attributed to the network analyzer. This procedure was not applied for frequencies beyond 1 GHz since the interpretation of that data would be too questionable.

Finally, the corrected S-parameters were plugged first into the well known "standard" logarithmic formula [1] for distributed impedance ($S_{21}$ and $Z$ are complex and $Z_c$ is real).

$$Z = -2\,Z_c\ \ln\frac{S_{21}}{S_{21\,ref}} \tag{3}$$

or

$$\begin{aligned} \mathrm{Re}[Z] &= -2\,Z_c\ \ln|\frac{S_{21}}{S_{21\,ref}}| \\ \mathrm{Im}[Z] &= -2\,Z_c\ \mathrm{phase}(S_{21}/S_{21\,ref}) \end{aligned} \tag{4}$$

The results of these calculations are shown on the Figs. 9-11 together with results obtained from the more accurate formula discussed below. A reference measurement in a smooth, homogeneous beam

pipe was not done here for practical reasons. Instead, we assumed for the reference a lossless line of length $l$.

We have noticed several high-Q resonances which are probably modified cavity resonances between the tank and the kicker module. This kicker module does not have (yet) short direct connections to the end of the tank and the cold conductor in the ferrite module. Thus cavity resonances are easily excited by the beam passing through the gaps on each side of the ferrite module.

## 2 Evaluation of a Distributed Impedance from Measured S-parameters

For the matched line (when the characteristic impedance is equal to the reference impedance) the only nonzero scattering parameter is [2]

$$S_{12} = \mathrm{e}^{-ikl},$$

where the propagation constant $k$ becomes:

- for the device under test (DUT)

$$k_D = \omega\sqrt{(1 - i\frac{R_0 + \zeta}{\omega L_0})L_0C_0},$$

- for the reference (REF) line

$$k_R = \omega\sqrt{(1 - i\frac{R_0}{\omega L_0})L_0C_0}.$$

The characteristic impedance of the reference line is

$$Z_c = \sqrt{\frac{\omega L_0 - iR_0}{\omega_0 C_0}}.$$

From the expressions above, the longitudinal impedance of the DUT can be written as [2]

$$Z = \zeta l = iZ_c\frac{(k_D^2 - k_R^2)l}{k_R} = Z_c \ln\frac{S_{12}^R}{S_{12}^D}(1 + \frac{\ln S_{12}^D}{\ln S_{12}^R}). \tag{5}$$

In our case, for a reference line without losses, $R_0 = 0$ and

$$S_{12}^R = \mathrm{e}^{i\phi_R},$$

where $\phi_R = -\frac{\omega}{c}l$.

If we define the DUT scattering parameter as

$$S_{12}^D = |S_{12}^D|\mathrm{e}^{i\phi_D},$$

then from Eq. (5) we have for the real part of impedance:

$$\mathrm{Re}[Z] = -2Z_c \ln|S_{12}^D|\,\frac{\phi_D}{\phi_R} = -2Z_c \ln|S_{12}^D|\,(1 + \frac{\Delta\phi}{\phi_R}), \tag{6}$$

where $\Delta\phi = \phi_D - \phi_R$.

From Figs. 9-11 we see that for frequencies above 100 MHz we obtain

$$\frac{\Delta\phi}{\phi_R} \simeq 1.$$

| $k$ | Freq. (MHz) | Re$(Z)$ $(\Omega)$ standard log formula | improved log formula |
|---|---|---|---|
| 0 | 0 | 0 | 0 |
| 1 | 200 | 640 | 950 |
| 2 | 400 | 1750 | 3500 |
| 3 | 600 | 1350 | 2490 |
| 4 | 800 | 1870 | 3710 |
| 5 | 1000 | 2740 | 5610 |

Table 1: Real part of the longitudinal coupling impedance by the standard log formula and the improved log formula.

Then the the more accurate formula (6) gives $\mathrm{Re}[Z]$ approximately a factor 2 higher in comparison with the "standard" log formula (3), which in fact is valid only for the case when the difference between DUT and REF impedances is not large [1]. Below 100 MHz the difference in results obtained from these 2 formulae is less significant.

For the imaginary part of the DUT impedance we obtain from Eq. (5)

$$\mathrm{Im}[Z] = -2Z_c\Delta\phi(1+\frac{\Delta\phi}{2\phi_R}) + Z_c\frac{\ln^2|S_{12}^D|}{\phi_R}. \tag{7}$$

The last term here is relevant only at very low frequencies. The difference in results obtained with this formula and the log formula (4) is smaller than for the real part of the impedance. For frequencies below 100 MHz the more accurate formula (7) gives an imaginary part of the coupling impedance about $15\%$ higher and above 100 MHz the average increase is around $50\%$.

The real part of the coupling impedance by the standard log formula and the improved log formula is shown in Table 1.

It should be noticed that applying the improved log formula (5) which returns a significantly higher real part as compared to the standard log formula when the measued S-parameters show more than about 10 dB attenuation, can also lead to surprises. For example consider the negative real part in Figs. 9 and 10 around 7 MHz. This is of course an unphysical result which may occur for certain "forbidden" ranges of amplitude and phase of the measured S-parameter. These ranges are dependent on the relative electrical length of the device under test and become in particular visible when using the improved log formula for short (as compared to the free space wavelength) DUTs. This effect is not caused by an incorrect S-parameter measurement, but simply by the fact that the physical reality does not correspond to what is assumed in the model (e.g. physical reality = lossy line + resonator; mode = lossy line only.) Related aspects are also treated in [3] and ranges of validity of the different formulae have been investigated graphically in [4]. Negative real parts may occur as well when applying the lumped element model where this not appropriate, even if the amplitude of $S_{21}$ is smaller than unity. The correlation of the real part of the impedance with results obtained from different numerical and analytical calculations given in [5] as well as heating data (towards the end of this note) leads to the following assumption: The real part (improved log formula) shown in Fig. 11 is reasonably close (within a factor of about 2) to what we may consider the true real part of the longitudinal impedanace. As for the imaginary part, using a similar reasoning this may be acceptable to about 400-500 MHz. The imaginary part of the MKE kicker impedance, evaluated from the measured S-parameters shown in Fig. 8 exhibits rather large values for frequencies higher than about 400 MHz. If these values were considered to be true, they would violate the condition that real and imaginary part of the impedance for this kind of structures are mutually dependent and to a certain extent can be deduced from each other. The frequency limit, given here is deduced from numerical simulations described in [5].

## 3 General Expressions for the Beam Spectrum

In the time domain, a beam current of $M$ identical bunches separated in time by $t_{bb}$ can be written in the form

$$J(t) = \sum_{n=0}^{M-1} j(t - nt_{bb}) = \sum_{k=-\infty}^{\infty} J_k e^{\frac{-i2\pi kt}{T_0}}, \tag{8}$$

where $j(t)$ is a single bunch current and $T_0$ is the revolution period.

In the frequency domain Fourier harmonics of the beam current are defined by the expression

$$J_k = \frac{1}{T_0} \int_{-T_0/2}^{T_0/2} \sum_{n=0}^{M-1} j(t - nt_{bb}) e^{\frac{i2\pi kt}{T_0}} dt, \tag{9}$$

Then we can write

$$J_k = j_k \sum_{n=0}^{M-1} e^{\frac{i2\pi knt_{bb}}{T_0}}, \tag{10}$$

where

$$j_k = \frac{1}{T_0} \int_{-T_0/2}^{T_0/2} j(t) e^{\frac{i2\pi kt}{T_0}} dt. \tag{11}$$

For a uniform distribution of bunches over the ring the beam spectrum contains only multiples of the bunch spacing frequency $1/t_{bb}$. After summation in (10), the spectrum of the beam with a gap ($M < T_0/t_{bb}$) can be presented as

$$J_k = j_k \frac{\sin M\xi_k}{\sin \xi_k} e^{i(M-1)\xi_k}, \tag{12}$$

where $\xi_k = \pi k t_{bb}/T_0$.

Below, for estimations, the bunch current is assumed to have the form

$$j(t) = \begin{cases} j_p \cos^2 \frac{\pi t}{\tau}, & -\tau/2 < t < \tau/2 \\ 0, & \text{elsewhere,} \end{cases} \tag{13}$$

where $\tau$ is the bunch length in seconds. A peak current $j_p = 2N_b e/\tau$ is defined by the normalization condition

$$eN_b = \int_{-T_0/2}^{T_0/2} j(t) dt,$$

where $N_b$ is the number of particles per bunch.

For the chosen bunch shape we have

$$j_k = \frac{j_p}{2\pi k} \frac{\sin \pi\alpha_k}{(1 - \alpha_k^2)} \tag{14}$$

with $\alpha_k = k\tau/T_0$.

Finally for the bunch shape (13) we have from (12)

$$J_k = J_A \frac{\sin \pi\alpha_k}{\pi\alpha_k(1 - \alpha_k^2)} \frac{\sin M\xi_k}{M \sin \xi_k} e^{i(M-1)\xi_k}, \tag{15}$$

where $J_A = MN_b e/T_0$ is the average beam current.

| $k$ | Freq. (MHz) | $\lvert J_{kh}/J_A\rvert$ t = 1.5 sec | $\lvert J_{kh}/J_A\rvert$ t = 4 sec | $\overline{\lvert J_{kh}/J_A\rvert}$ | $\overline{\lvert J_{kh}/J_A\rvert}$ (cable loss corrected) |
|---|---|---|---|---|---|
| 1 | 200 | 0.90 | 0.93 | 0.915 | 0.912 |
| 2 | 400 | 0.59 | 0.67 | 0.63 | 0.67 |
| 3 | 600 | 0.38 | 0.44 | 0.41 | 0.46 |
| 4 | 800 | 0.22 | 0.26 | 0.24 | 0.28 |
| 5 | 1000 | 0.1 | 0.093 | 0.1 | 0.13 |

Table 2: Bunch spectra of the SPS at $J_A = 132$ mA.

## 4 Fixed Target Proton Beam in the SPS

In the case of the fixed target proton beam in the SPS, 10/11 of the ring are filled with 5 ns spaced bunches. For a uniform distribution of bunches over the ring, the beam spectrum contains lines only at multiples of the bunch spacing frequency $1/t_{bb} = 200$ MHz. At injection, assuming a bunch length of 4 ns, the envelope of the spectrum $|J_k|/J_A$ corresponding to the bunch distribution (13) has the form presented in Fig. 12 (right).

The existence of the gap gives additional lines at revolution frequency harmonics. Their envelope, described by expression $J_k/(Mj_k)$ in formula (12), is shown in Fig. 12 (left) around the main 200 MHz line. (For this type of beam, parameter $\xi_k = \pi k/4620$ and $M\xi_k = \pi k 10/11$).

During the acceleration cycle, the beam spectrum is varying due to bunch length and particle distribution changes. The last happens for a high intensity beam as a result of longitudinal instabilities.

Assuming that particle distribution and longitudinal emittance stay constant during the cycle, the envelope of the beam spectrum at the end of the cycle is presented in Fig. 12 (right). In this case the bunch length changes with time according to the curve shown in Fig. 13 (left). The variation during the cycle of the RMS beam spectrum components

$$J_k^{rms} = \sqrt{2} J_k$$

is shown in Fig. 13 (right) for multiples of RF harmonics $k = h, 2h, 3h...$ and for a total beam intensity in the ring of $10^{13}$ ($J_A = 69.4$ mA). However this is valid only for a beam with total intensity at or below $10^{13}$, [6]. For higher intensity beams, the bunch length does not decrease after transition crossing as is shown in Fig. 13, due to continuous emittance blow-up, see the bunch length measurement in [6]. For the highest total intensities reached in the SPS till now ($4.7 \times 10^{13}$) during normal operation cycle, the longitudinal emittance increases by a factor 10 and the effective bunch length corresponding to the particle distribution (13) is about 3 ns. For this value of bunch length the beam spectrum envelope $|J_k|/J_A$ is shown in Fig. 14 (left). In Fig. 14 (right) the beam spectrum envelope is calculated for the bunch length of 1.7 ns which corresponds to the total intensity of $2 \times 10^{13}$.

Table 2 gives the average bunch spectrum components, taken from measurements of the beam spectrum at different moments in the cycle with a linear power averaging applied. Note that these measured spectral intensities are only used in relative terms in order to determine the best fit bunch length, but not for an absolute spectral power reading.

## 5 Comparison of Power Dissipation Estimates and Heating Caused by the SPS Beam

The power dissipated in the kicker can be calculated with the following equation:

$$P = \eta |J_A|^2 \sum_{k=-\infty}^{\infty} \mathrm{Re}(Z(k\omega_0)) |J_k/J_A|^2, \tag{16}$$

where $\eta$ is the duty factor. Now we assume the impedance $Z$ is broadband, and add the contributions of the sidebands

$$\sum_{k=0}^{h-1}\left|\frac{\sin(M\xi_k)}{M\sin(\xi_k)}\right|^2 = \frac{h}{M}.$$

Thus the power is

$$P \simeq 2\eta|J_A|^2\frac{h}{M}\sum_{k=1}^{5}\mathrm{Re}(Z(kh\omega_0))|J_{kh}/J_A|^2. \tag{17}$$

We apply this formula to the SPS MKE kicker. There was a measurement at $J_A$ = 132 mA, and the measured power is 60 W [7]. The power is

$$P = \begin{cases} 17\,W, & \text{standard log formula} \\ 30\,W, & \text{improved log formula} \end{cases} \tag{18}$$

where we used $\eta = 0.243$.

## 6 Conclusion

The heat load estimated from the measured real part of the MKE impedance is smaller than that directly measured by a factor two. To interpret the raw data obtained by the wire method, both standard and improved log-formulae were used. The latter gives results closer to both the direct heat loss measurement and the impedance calculation using a numerical code [5] and as demonstrated should be used for distributed impedances which are large in comparison with the impedance of the reference line. For a realistic heat loss estimation it was also important to use the measured spectral components and not those calculated since at an intensity of $2 \times 10^{13}$ the fixed target beam is unstable, leading to significant emittance blow-up. The heat load and impedance, (from Fig. 10, the low frequency inductive part is Im[Z]/n = 0.43 $\Omega$ per kicker), are not negligible and possible ways to reduce them should be investigated.

## Acknowledgements

Many thanks to T. Linnecar for useful discussions, T. Bohl for the SPS signal cable attenuation measurement, J. G. Bertin and J. C. Guillot for preparing the bench set-up, D. Brandt for helpful comments, and E. Jensen for further studies of distributed impedances.

## References

[1] L.S.Walling et al, “Transmission line impedance measurements for an Advance Hadron Facility”, NIM, A 281, 1989, p.433.

[2] V.Vaccaro, “Coupling impedance measurements: an improved wire method”, INFN/TC-94/023, 1994.

[3] H. Hahn, M. Morvillo, A. Ratti, “The Coupling Impedance of the RHIC Injection Kicker”, AD/RHIC/RD-95, 1995.

[4] E. Jensen, “An Improved Log-formula for Homogeneously Distributed Impedance”, PS/RF/Note 2000-001, 2000.

[5] H. Tsutsui, “Some Simplified Models of Ferrite Kicker Magnet for Calculation of Longitudinal Impedance”, CERN-SL-2000-004 AP, 2000.

[6] T.Bohl, T.Linnecar, E.Shaposhnikova, “Emittance control by the modification of the voltage programme”, CERN SL-MD Note 246, 1997.

[7] G. Schröder, private communication.

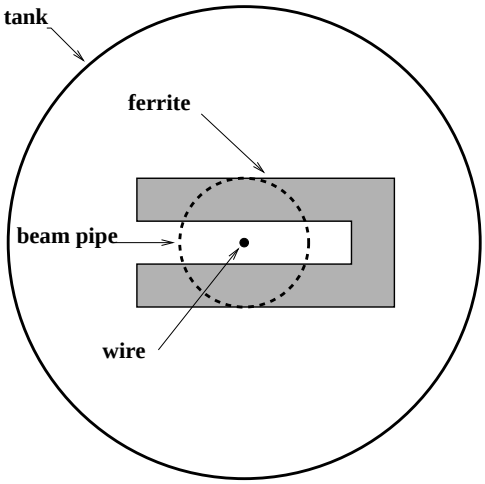


Figure 1: Simplified schematic cross-section of the MKE kicker (vertical aperture: 32 mm, horizontal aperture: 140 mm, wire diameter: 0.4 mm).

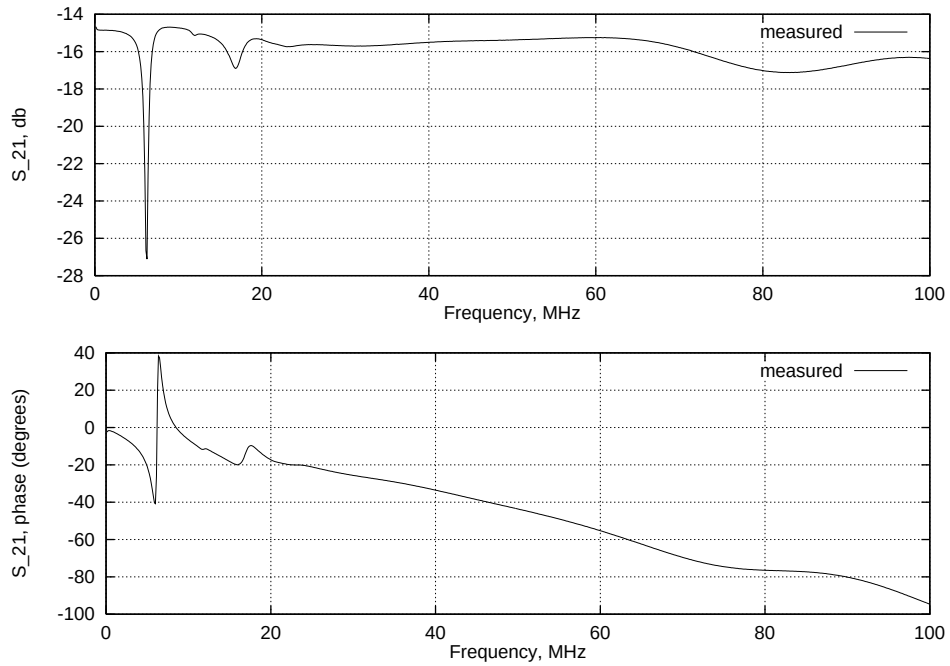


Figure 2: Raw data: amplitude and phase in the frequency range up to 100 MHz from a network analyzer with mechanical correction $l = 2.2253$ m taken into account, and cable calibration done.

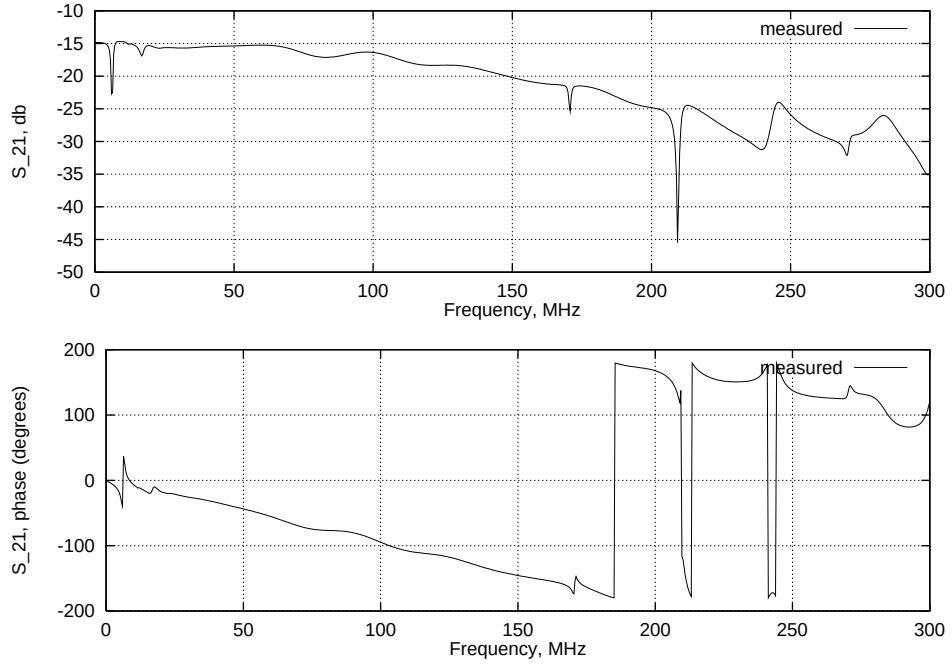


Figure 3: Raw data: amplitude and phase in the frequency range up to 300 MHz from a network analyzer with mechanical correction $l = 2.2253$ m taken into account, and cable calibration done.

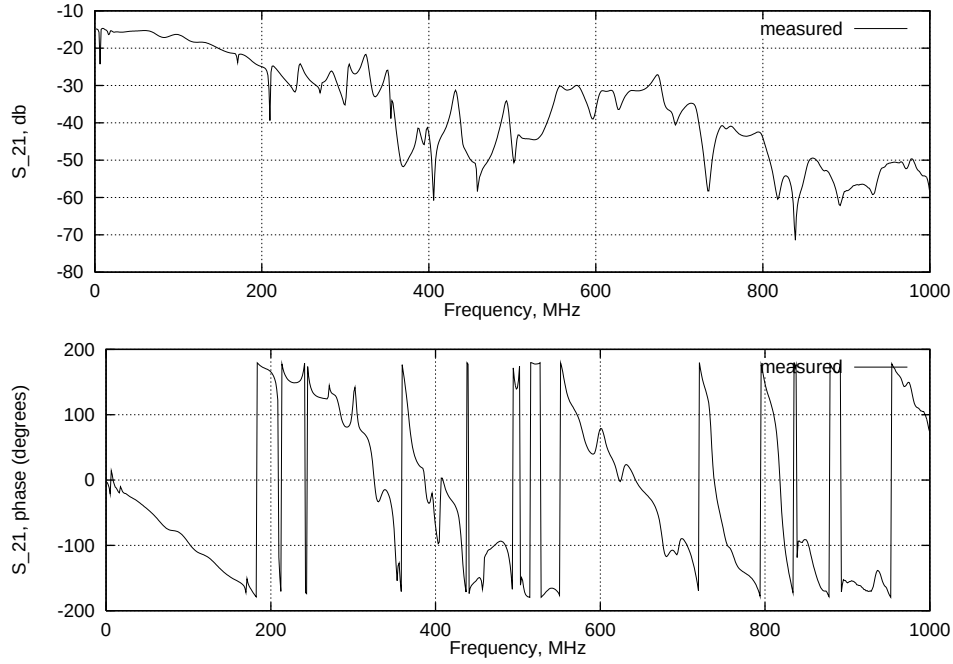


Figure 4: Raw data: amplitude and phase in the frequency range up to 1000 MHz from a network analyzer with mechanical correction $l = 2.2253$ m taken into account, and cable calibration done.

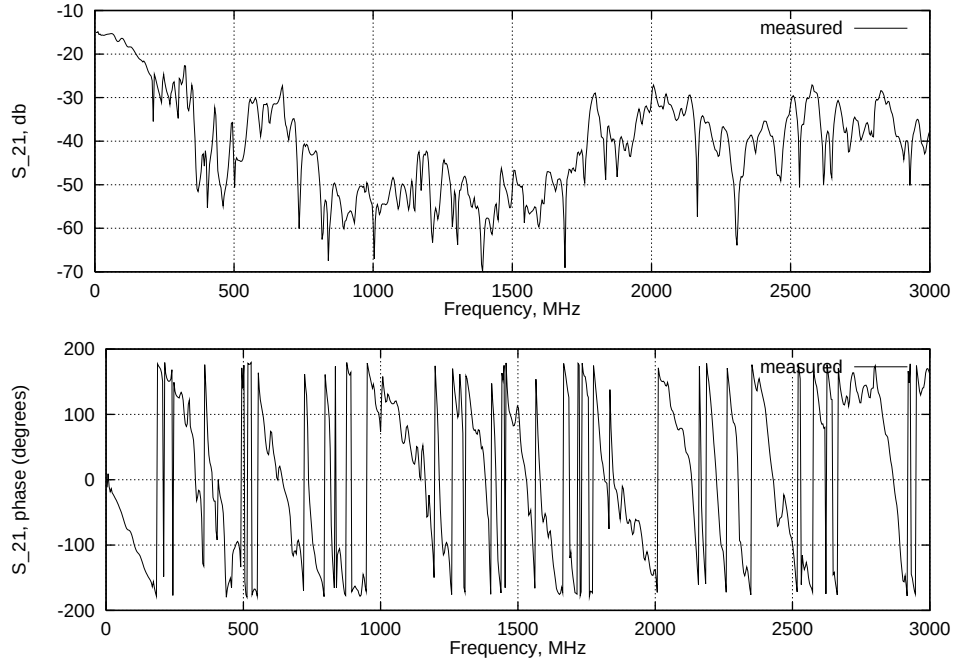


Figure 5: Raw data: amplitude and phase in the frequency range up to 3000 MHz from a network analyzer with mechanical correction $l = 2.2253$ m taken into account, and cable calibration done.

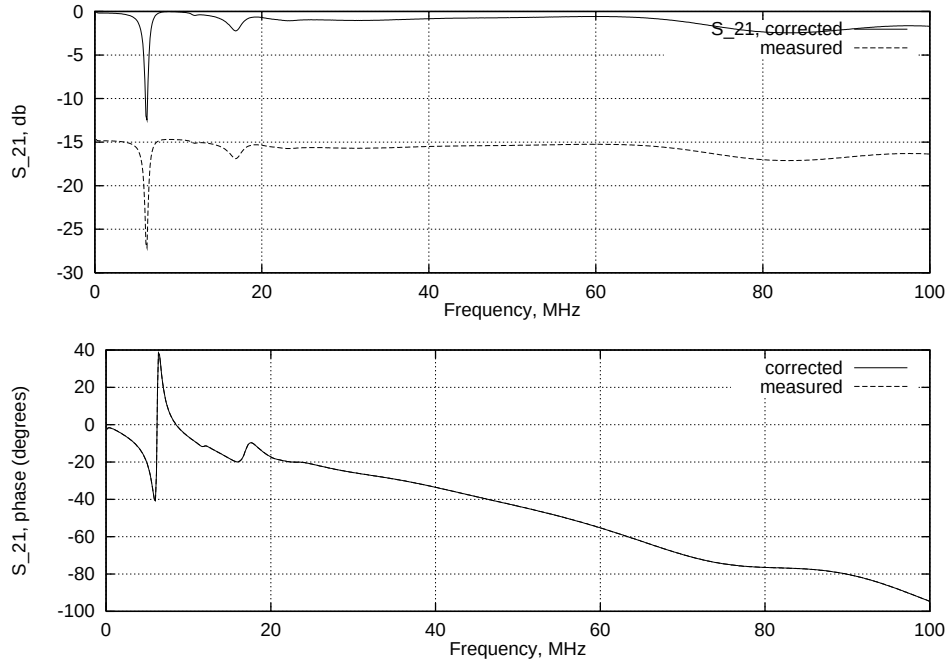


Figure 6: Corrected S-parameters: the losses from the matching resistors are taken into account, and the phase ambiguity related $360^\circ$ jumps are removed.

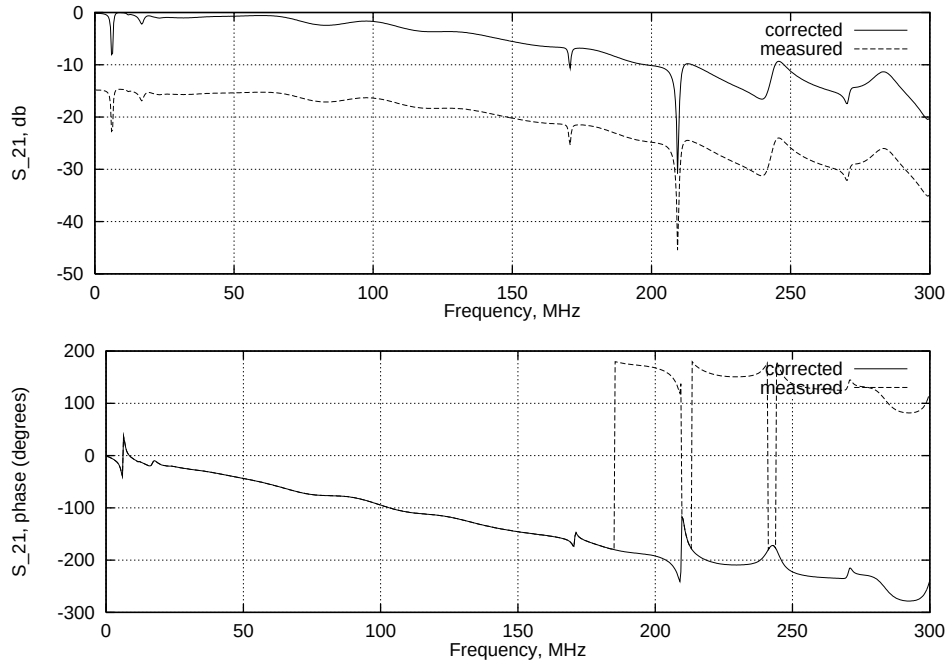


Figure 7: Corrected S-parameters: the losses from the matching resistors are taken into account, and the phase ambiguity related $360^\circ$ phase jumps are removed.

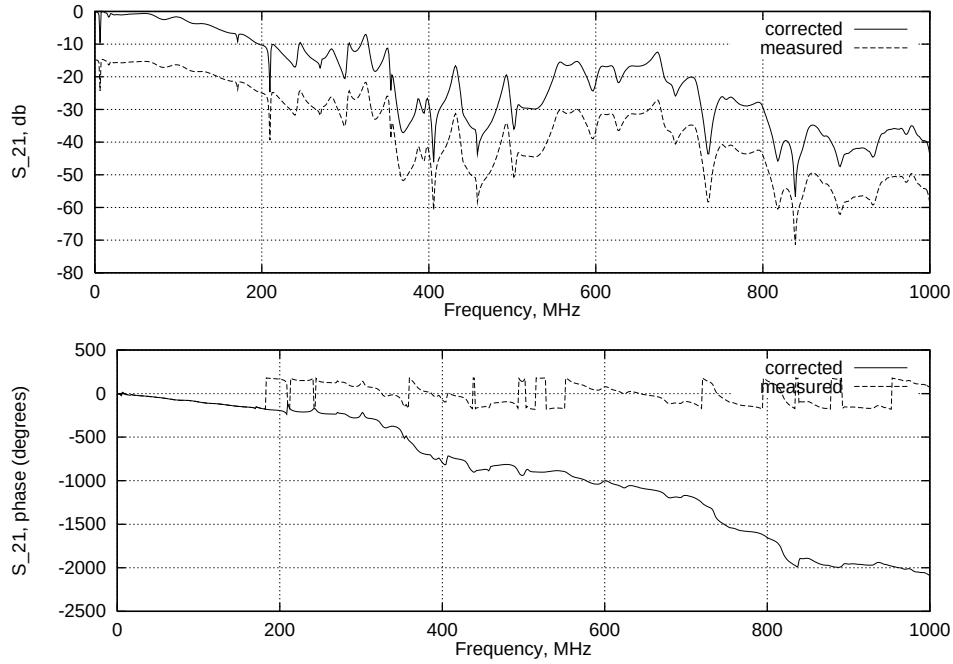


Figure 8: Corrected S-parameters: the losses from the matching resistors are taken into account, and the phase ambiguity related $360^\circ$ jumps are removed.

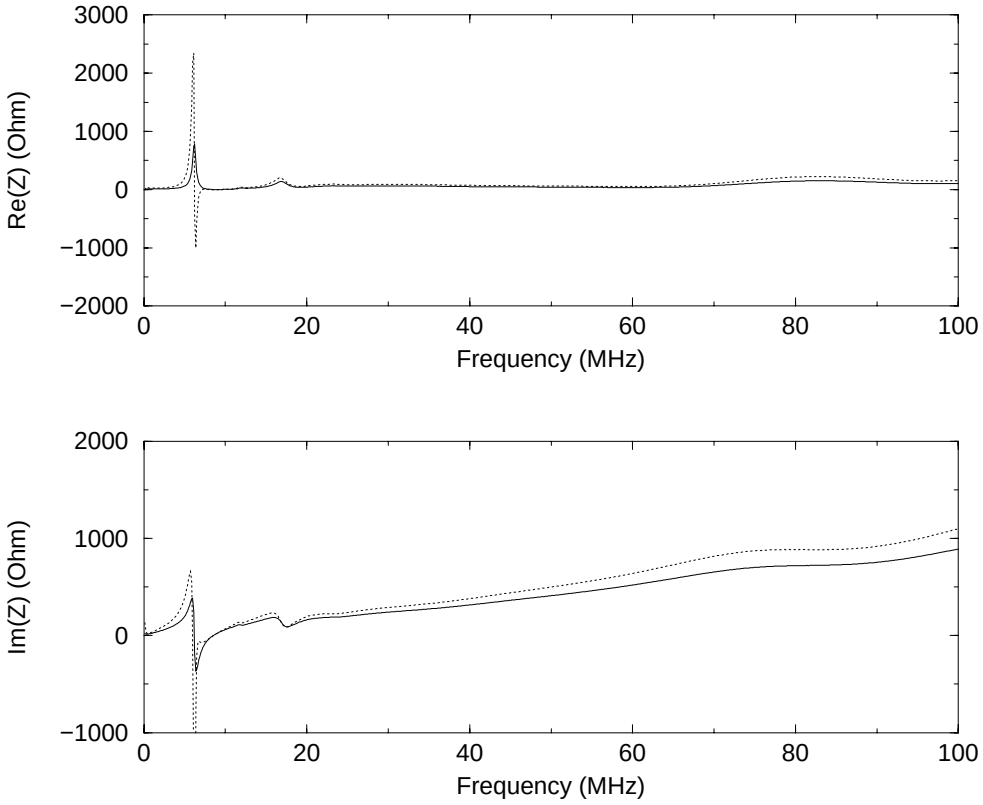


Figure 9: Impedances calculated from the corrected values of amplitude and phase of $S_{21}$. Solid and dotted lines show the result by standard log formula and improved log formula, respectively. Note the negative real part (unphysical result) around 7 MHz from the improved log formula.

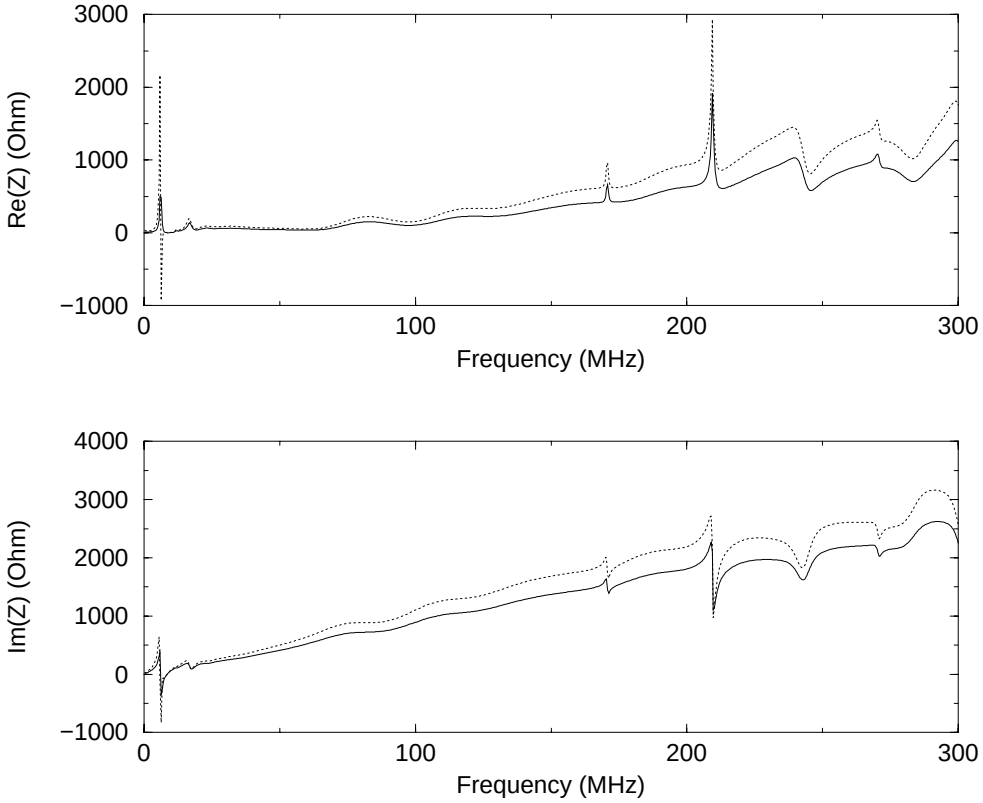


Figure 10: Impedances calculated from the corrected values of amplitude and phase of $S_{21}$. Solid and dotted lines show the result by standard log formula and improved log formula, respectively.

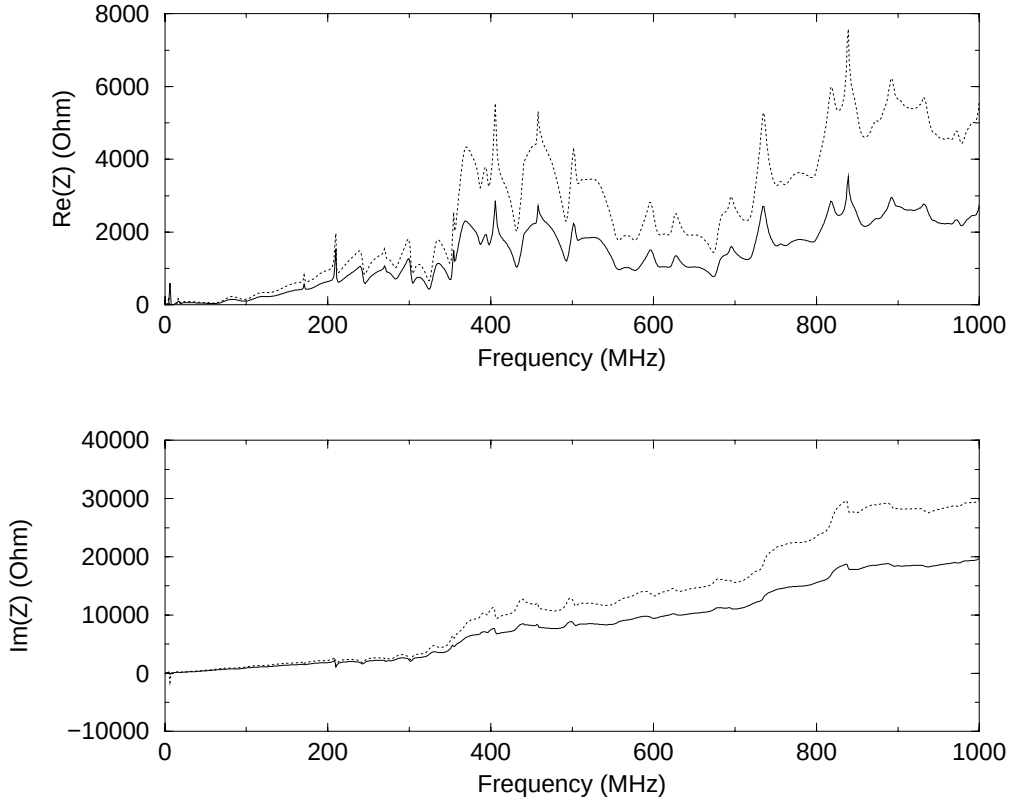


Figure 11: Impedances calculated from the corrected values of amplitude and phase of $S_{21}$. Solid and dotted lines show the result by standard log formula and improved log formula, respectively.

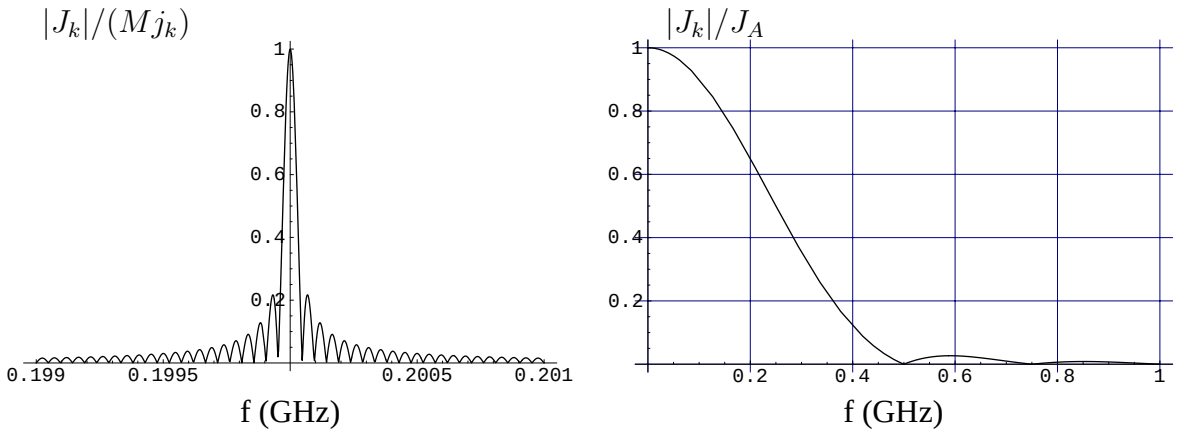


Figure 12: Left: fine structure of the beam spectrum around 200 MHz line. Right: beam spectrum envelope for a 4 ns bunch length (at injection).

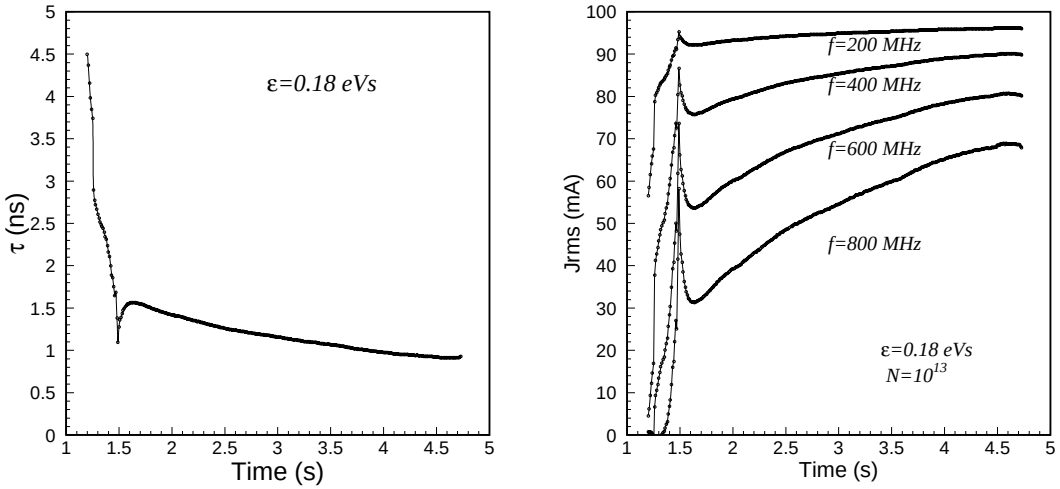


Figure 13: Left: bunch length for low intensity beam during SPS fixed target proton cycle in normal operation. Right: beam spectrum components during SPS fixed target cycle in normal operation for beam intensity $10^{13}$.

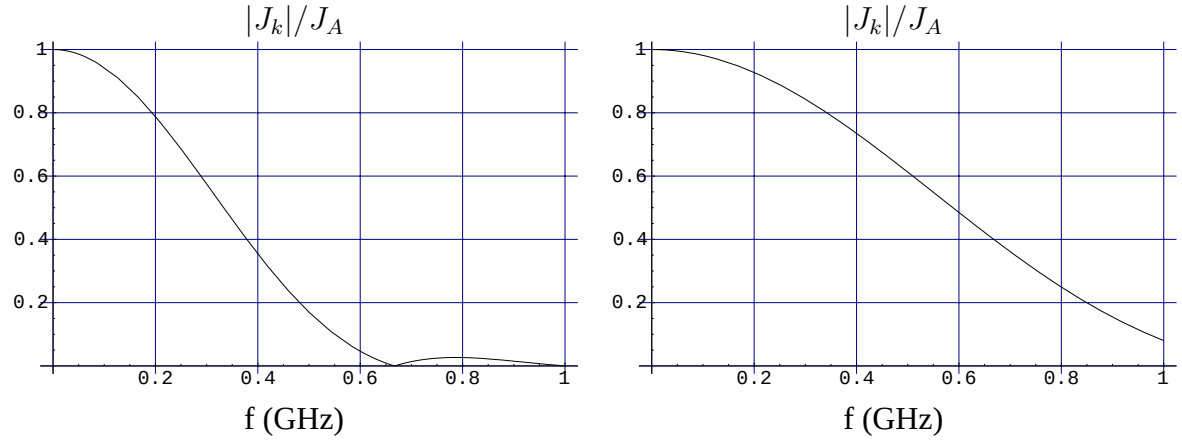


Figure 14: Spectrum for the beam with bunch length of 3 ns (left) and 1.7 ns (right).